

Extended Theory on the Inductance Calculation of Planar Spiral Windings Including the Effect of Double-layer Electromagnetic Shield

Y. P. Su, Xun Liu and S. Y. (Ron) Hui

Center for Power Electronics
City University of Hong Kong
Tat Chee Avenue, Kowloon
Hong Kong, China
(email: eeronhui@cityu.edu.hk)

Abstract - Recent progress on wireless planar battery charging platform highlights a requirement that the platform must be shielded underneath so that the electromagnetic (EM) flux will not leak through the bottom of the charging platform. The presence of the EM shield will inevitably alter the flux distribution and thus the inductance of the planar windings. In this paper, a theory of calculating inductance of spiral windings is extended to determine the inductance of planar spiral windings shielded by a double-layer planar EM shield. With the generalized equations, the impedance of the planar spiral windings on double-layer shielding substrate and the optimal thickness of shielding materials can be calculated accurately without using time-consuming finite-element method. Therefore, the influence of the double-layer electromagnetic shield on the inductance of the planar spiral windings can be analyzed. Simulations and measurements have been carried out for several shielding plates with different permeability, conductivity and thickness. Both of the simulations and measurements of the winding inductance agree well with the extended theory.

Keywords - planar spiral inductance, double-layer shield, impedance formulas

NOMENCLATURE

a_1, r_1	Internal radii of circular winding.
a_2, r_2	External radii of circular winding.
d_1, d_2	Height of filaments or winding centers above the substrate.
h_1, h_2	Thickness of the winding track.
$J_0(x), J_1(x)$	Bessel functions of the first kind.
L_0	Self-inductance of windings in air.
L_1	Self-inductance with single-layer substrates.
L_2	Self-inductance with double-layer substrates.
L_s	Additional inductance of windings due to the presence of substrate.
M	Mutual inductance between two windings or filaments in air.
Q, S	Defined in (4) and (5).
R_s	Additional resistance of windings due to eddy loss in substrate.

t_1, t_2	Substrates thickness.
Z	Mutual impedance between two windings or filaments.
Z_i^f	Additional mutual impedance due to presence of substrates.
ω	Angular frequency (rad/s).
σ_1, σ_2	Electrical conductivity of the substrates.
μ_{r1}, μ_{r2}	Relative permeability of the substrates.
μ_0	Permeability of free space ($4\pi \times 10^{-7} H / m$).
$\lambda(t_1, t_2)$	Defined in (6).
$\phi_1(k), \phi_2(k)$	Defined in (7) and (8).
$m, \theta(t_2)$	Defined in (9) and (10).
η_1, η_2	Defined in (11) and (12).

I. INTRODUCTION

Inductance calculation methods for spiral planar windings [1,2] have provided a useful tool for researchers to investigate various applications of planar windings. Planar magnetic components are attractive in portable electronic equipment applications in which high power density and slim designs are preferred. For examples, coreless planar transformers for signal and power transfer have been studied [3,4]. The loss modeling of planar inductor for thermal management has also been investigated [5]. Planar spiral windings have been used for gate drive applications [6] and stray inductance cancellation in EMI filter [7-9]. Recent industrial applications of planar windings include stand-alone battery chargers [10] and induction heating [11-13]. The inductance calculation of spiral windings with variable widths is reported in [14].

So far, the inductance of planar spiral windings on a single-layer substrate of finite thickness or in a sandwich structure has been analyzed [1,2,15]. However, it has been shown that a patented double-layer EM shield consisting of a soft-magnetic plate and a conducting plate can achieve a much higher shielding effectiveness [16]. This double-layer EM shield structure is particularly important for designing planar wireless charging platform [17] because the platform must be shielded underneath so that the magnetic flux will not leak through the

bottom of the platform. However, the presence of the EM shield will affect the inductance of the planar windings.

In this paper, an extended theory based on the equations in [1,2] for calculating inductance of spiral windings is presented. A new set of formulas have been developed to calculate the inductance of planar spiral windings with double-layer planar EM shield. This extended theory can be used to optimize the spiral windings and EM shield design. In this project, it is used to choose proper shielding parameters for the universal wireless battery the platform. With the generalized equations presented in this paper, the mutual impedance of the planar spiral windings on double-layer shielding substrate structure and the optimal thickness of shielding materials can be calculated directly without using time-consuming finite-element software. The frequency dependent losses, particularly due to eddy currents in magnetic substrate, have also been considered in the calculation. Theoretical results agree favorably with the finite-element simulation results and practical measurements for several ferrite plates with different permeability and thickness. This extended theory also leads to some interesting discoveries that are useful to the optimal design of the shielding structure, such as the optimal thickness of the ferrite plate.

II. IMPEDANCE FORMULA

A set of frequency-dependent impedance formulas for planar spiral windings on a magnetic substrate of finite thickness or a planar coils sandwiched between two magnetic substrates are reported in [1,2]. Such theory considers the non-uniform current distribution in planar coils and the loss in magnetic media. The impedance formulas are derived from Maxwell's equations. In the first step of deduction in this theory, the formula of the mutual inductance between two filaments is reproduced in [1]. Then the mutual inductance between two planar windings is obtained by integrating the previous formulas over the cross-section of the conductor, taking the current density distribution into account and assuming that the variation over the height of the cross-section is negligible [1]. By extending the results in [1] and [2], a new set of impedance formulas are set up for planar spiral windings placed on a double-layered, planar EM shield constructed with a ferrite plate and a copper plate.

Fig. 1 and Fig. 2 show the 3-D view and cross-sectional view of two turns of concentric circular windings on a double-layered substrate having relative permeability of μ_{r1}, μ_{r2} , electrical conductivity of σ_1, σ_2 and thickness of t_1, t_2 , respectively. The mutual impedance between the two windings is given by (1)

$$Z = j\omega M + Z_i^f \quad (1)$$

where M is the mutual inductance which would exist in the absence of the substrate and can be calculated by (2); Z_i^f is the additional impedance due to the presence of the double-layered substrate and can be calculated by (3). The real part of Z_i^f , the resistive component, represents the losses due to the eddy currents in the substrate, and the imaginary part of Z_i^f , the

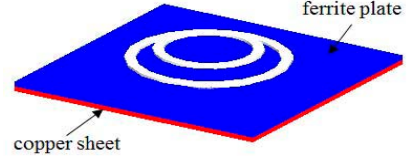


Fig. 1. 3-D view of the model of planar windings on double-layer substrate

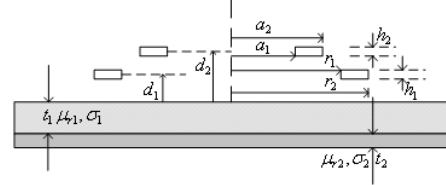


Fig. 2. cross-sectional view in R-Z plane of the model of planar windings on double-layer substrate

inductive reactance, enhances the inductance in the air. The specific definitions of nomenclature are given below:

$$M = \frac{\mu_0 \pi}{h_1 h_2 \ln\left(\frac{r_2}{r_1}\right) \ln\left(\frac{a_2}{a_1}\right)} \int_0^\infty S(kr_2, kr_1) S(ka_2, ka_1) Q(kh_1, kh_2) e^{-k|d_2-d_1|} dk \quad (2)$$

$$Z_i^f = \frac{j\omega \mu_0 \pi}{h_1 h_2 \ln\left(\frac{r_2}{r_1}\right) \ln\left(\frac{a_2}{a_1}\right)} \int_0^\infty S(kr_2, kr_1) S(ka_2, ka_1) Q(kh_1, kh_2) \lambda(t_1, t_2) e^{-k(d_1+d_2)} dk \quad (3)$$

$$\text{where } Q(kx, ky) \begin{cases} = \frac{2}{k^2} \left[\cosh k \frac{x+y}{2} - \cosh k \frac{x-y}{2} \right], z > \frac{h_1+h_2}{2} \\ = \frac{2}{k} \left(h + \frac{e^{-kh} - 1}{k} \right), z = 0, x = y = h \end{cases} \quad (4)$$

$$S(kx, ky) = \frac{J_0(kx) - J_0(ky)}{k} \quad (5)$$

$J_0(kx)$ is a Bessel Function of the first kind.

Due to the new double-layered substrate, the parameter function $\lambda(t_1, t_2)$ in (3) has a modified expression as shown below:

$$\lambda(t_1, t_2) = \frac{\phi_1(k) + \frac{\theta(t_2) - m}{\theta(t_2) + m} e^{-2\eta_1 t_1}}{1 + \phi_1(k) \frac{\theta(t_2) - m}{\theta(t_2) + m} e^{-2\eta_1 t_1}} \quad (6)$$

where $\phi_1(k)$, $\phi_2(k)$, m , $\theta(t_2)$ are defined in (7), (8), (9) and (10), respectively.

$$\phi_1(k) = \frac{\mu_{r1} - \frac{\eta_1}{k}}{\mu_{r1} + \frac{\eta_1}{k}} \quad (7)$$

$$\phi_2(k) = \frac{\mu_{r2} - \frac{\eta_2}{k}}{\mu_{r2} + \frac{\eta_2}{k}} \quad (8)$$

$$m = \frac{\mu_{r1}\eta_2}{\mu_{r2}\eta_1} \quad (9)$$

$$\theta(t_2) = \frac{1 - \phi_2(k)e^{-2\eta_2 t_2}}{1 + \phi_2(k)e^{-2\eta_2 t_2}} \quad (10)$$

and

$$\eta_1 = \sqrt{k^2 + j\omega\mu_{r1}\mu_0\sigma_1} \quad (11)$$

$$\eta_2 = \sqrt{k^2 + j\omega\mu_{r2}\mu_0\sigma_2} \quad (12)$$

The derivation of these equations is given in the Appendix.

It is important to note that the above equations is an extended form of the calculation method presented in [1,2]. When the two layers are made of the same material,

$$\text{(i.e., } m = 1, \phi_1(k) = \phi_2(k) = \frac{\mu_r - \frac{\eta}{k}}{\mu_r + \frac{\eta}{k}} \text{)}, \text{ the new parameter}$$

function $\lambda(t_1, t_2)$ of (6) can be simplified to (13) as follows:

$$\lambda(t_1, t_2) = \frac{\phi_1(k)(1 - e^{-2\eta(t_1+t_2)})}{1 - \phi_1^2(k)e^{-2\eta(t_1+t_2)}} \quad (13)$$

It can be seen that (1)-(3) is identical to the equations for spiral windings placed on a single-layered substrate of finite thickness as reported in [1]. Hence, the extended theory can be reduced to the original theory if a single-layer substrate is used.

III. VERIFICATION AND ANALYSIS

The formula is proposed universally for two turns of concentric circular windings on a double-layered substrate made of any materials. For an N-turn spiral coil, the total impedance is the summation of each mutual impedance pairs between two concentric circular windings:

$$Z_{sum} = \sum_{j=1}^N \sum_{i=1}^N Z_{ij} \quad (14)$$

where Z_{ij} is substitute to Z in (1).

A. Verification

To evaluate the validity of the formula presented, a prototype shown in Fig. 3 has been analyzed as an example. The spiral planar winding has 10 turns. The geometric parameters of the planar spiral winding and the double-layered shielding structure are illustrated in Fig. 3.

It can be seen in (6) that the parameter function $\lambda(t_1, t_2)$ depends on seven variables: the thickness t_1, t_2 , the relative permeability μ_{r1}, μ_{r2} , the conductivity σ_1, σ_2 , and the frequency ω , where subscripts 1 and 2 refer to the first-layer and the second-layer of the substrate, respectively. In the verification of the formula, the material of the first-layer plate is respectively assumed to be dielectric and ferrite (4F1) whose relative permeability is prominently different from each other ($\mu_{r_di} = 1, \mu_{r_Fe} = 80$). The influence of some other variables will be shown. The self-inductance of the spiral winding is presented by calculated results (MATLABTM), simulated results

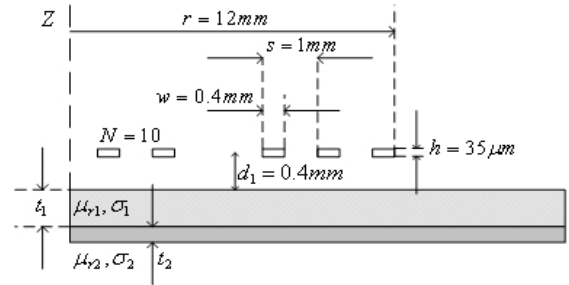


Fig.3. Cross-sectional view of the prototype in R-Z half plane

(AnsoftTM) and measured results in order to justify the formula. For clear comparison, all the results are normalized as ratio to the inductance of windings in the air (without substrate), $L_0 = 1.312\mu H$.

(i) First-layer of dielectric and second-layer of copper

Firstly, the case of using a double-layered substrate consisting of a dielectric such as PCB lamination material (FR4: $\mu_{r1} = 1, \sigma_1 = 0, \epsilon_{r1} = 4.4$), and copper is considered. Fig. 4(a) shows the inductance curve as a function of frequency while the thicknesses of the substrate are $t_1 = 0.3mm, t_2 = 0.03mm$. Fig. 4(b) shows the inductance curve as a function of frequency with the thickness of the copper layer changed to 0.06mm while other parameters remain unchanged.

Secondly, the case of inductance with double-layered substrate (dielectric and copper) as a function of t_1 is examined, t_1 is changed from 0mm-0.5mm and the operation frequency is chosen as 500 kHz. The results curve is shown in Fig. 5.

Although the case of substrate composed of dielectric and copper does not have many applications from a practical point of view, the results from calculation, simulation and measurement are highly consistent. This good agreement confirms the validity of the formula. The addition of the copper layer has a negative effect to the inductance of the spiral winding, especially when the relative permeability of the first layer is low.

(ii) First-layer of ferrite (4F1) and second-layer of copper

The case of using a double-layered substrate consisting of ferrite (4F1: $\mu_{r1} = 80, \sigma_1 = 1 \times 10^{-5} S/m$) and copper is then analyzed. Fig. 6(a) illustrates the inductance curve as a function of frequency while the thicknesses of the substrates are $t_1 = 0.5mm, t_2 = 0.03mm$. Fig. 6(b) illustrates the inductance curve as a function of frequency with the thickness of the copper layer changed to 0.06mm while keeping other parameters unchanged. These results show that the double-layered shield of ferrite and copper does not reduce the winding inductance significantly. However, the thin double-layered EM shield will provide a significant shielding effectiveness.

B. Analysis

For the purpose of enhancing the inductance and providing an effective EM shielding, the magnetic material, ferrite, is

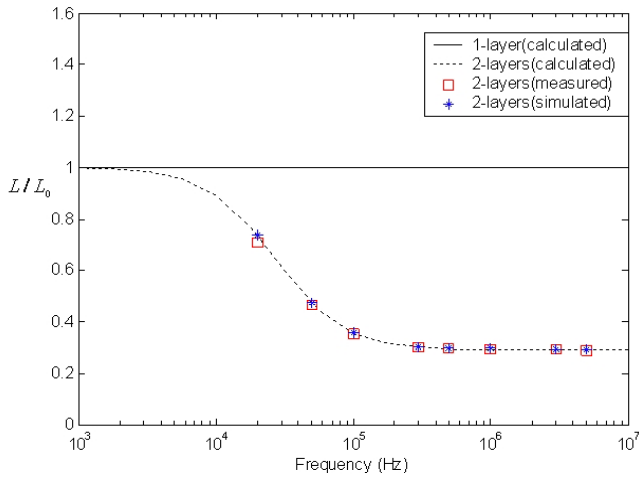


Fig. 4 (a) $t_1 = 0.3mm, t_2 = 0.03mm$

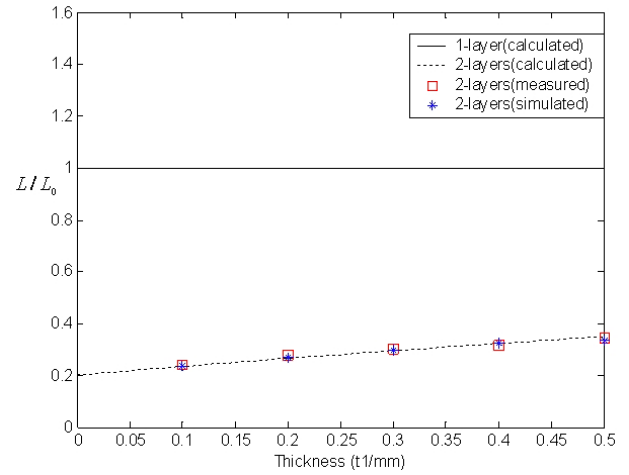


Fig. 5 Inductance with double-layer substrate (dielectric and copper) as a function of t_1 ; $f = 500KHz$; $t_2 = 0.03mm$; $L_0 = 1.312\mu H$

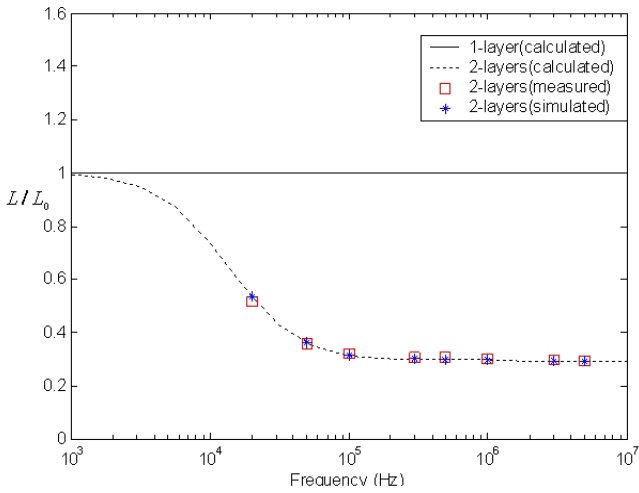


Fig. 4 (b) $t_1 = 0.3mm, t_2 = 0.06mm$

Fig. 4 Inductance with double-layer substrate (dielectric and copper) as a function of frequency; $L_0 = 1.312\mu H$

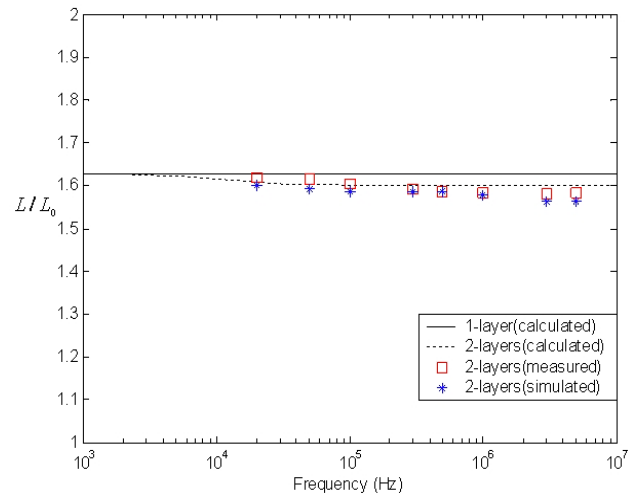


Fig. 6 (a) $t_1 = 0.5mm, t_2 = 0.06mm$

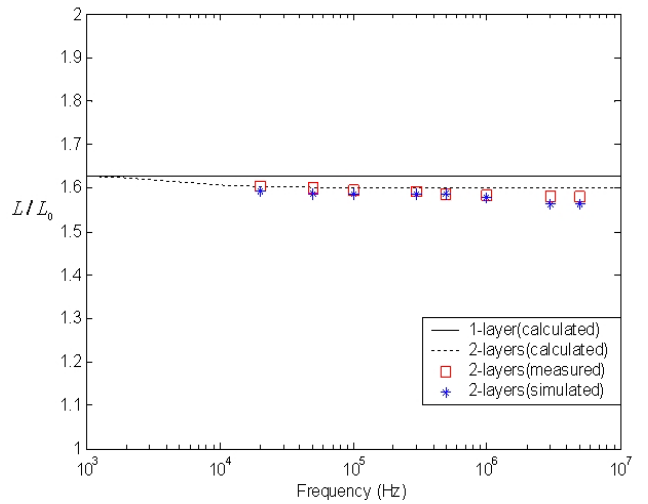


Fig. 6 (b) $t_1 = 0.5mm, t_2 = 0.06mm$

Fig. 6 Inductance with double-layer substrate (4F1 and copper) as a function of frequency; $L_0 = 1.312\mu H$

usually chosen as the material of the substrate. In this section, the calculation and simulation will be carried out with the same prototype shown in Fig. 3 and some of the calculation results will be given, when the thickness of the ferrite plate, t_1 , or the frequency, ω , changes. The result for double-layered shield is compared with that for single-layered shield (i.e. the copper sheet is absent), in order to highlight the effect of the copper sheet on the inductance of planar spiral windings.

(i) *thickness of the first layer, t_1 , changes*

Firstly, only the thickness of the ferrite plate is changed and the thickness of copper is fixed at $t_2 = 0.07mm$, while other parameters are unchanged and the frequency is fixed at 500 kHz. The calculated results are compared with finite-element simulated results in Fig. 7. All the results are normalized as a ratio to the inductance of windings in the air (without substrate), $L_0 = 1.312\mu H$. Fig. 7(a) and (b) show the results when the material of the ferrite plate is 4F1 ($\mu_{r1} = 80$) and

3F3 ($\mu_{r1} = 900$), respectively. Based on the theoretical results from the extended theory and the measurements, it can be seen that the extended theory can predict the optimal thickness of the ferrite plate for a given permeability. Both results in Fig.7(a) and Fig.7(b) indicate that the winding inductance can be enhanced if the thickness of the ferrite plate is larger than a certain value. If the ferrite plate is thick enough, the copper sheet has little influence on the inductance. But this additional copper sheet can greatly increase the shielding effectiveness.

If t_1 is larger than the critical value, this kind of negative effect of the copper layer on the winding inductance becomes negligible. For example, if we set L_2/L_1 to be greater than 0.97 as an indicator (so that L_2 is virtually the same as L_1), the thickness of the ferrite plate t_1 can be chosen to be 0.4mm for the case of ferrite 4F1 and 0.2mm for the case of ferrite 3F3. (Note that ferrite plates of 0.5mm are available in the market.) The critical thickness value decreases with increasing relative

permeability of the first layer of ferrite material.

(ii) frequency changes

A test has been performed to evaluate the frequency effects of the double-layered substrate on the inductance of planar spiral windings. The 4F1 ferrite plate is used in the test for a frequency range from 1kHz to 10MHz. Fig.8 (a) and (b) show the results when the thickness of the ferrite plate, t_1 , is 0.05mm and 0.4mm, respectively. If the thickness of the ferrite plate is less than the critical value, e.g. $t_1=0.2\text{mm}$ ($< 0.4\text{mm}$), the induced current in the copper sheet will incur power loss and thus reduce the winding inductance as the frequency increases, as shown in Fig.8(a). However, once the thickness of the ferrite is reached ($t_1=0.4\text{mm}$), the adverse effect of the copper sheet diminishes as confirmed in Fig.8(b).

The real part of Z_i^f which represents the eddy currents losses in the substrate is highly dependent on the operating frequency. In this double-layer case, the resistive element

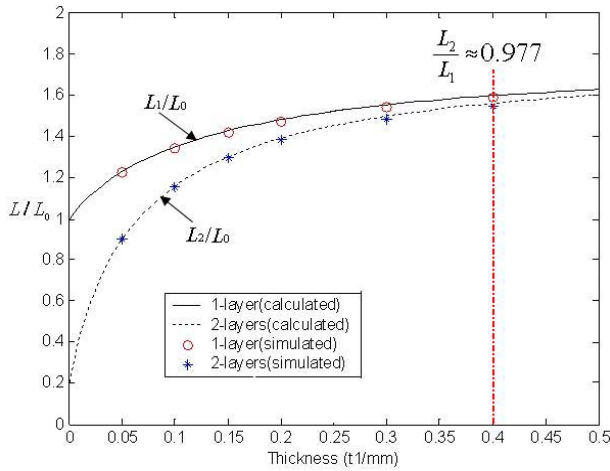


Fig. 7 (a) Ferrite plate 4F1 ($\mu_{r1} = 80, \sigma_1 = 1 \times 10^{-5} S/m$)

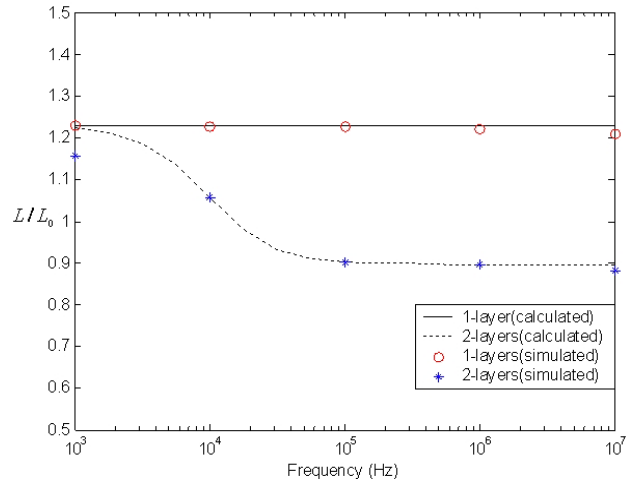


Fig. 8 (a) $t_1=0.05\text{mm}$

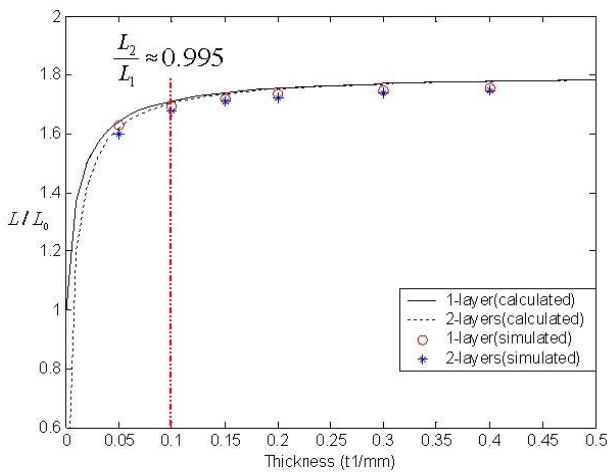


Fig. 7 (b) Ferrite plate 3F3 ($\mu_{r1} = 900, \sigma_1 = 0.1 S/m$)

Fig. 7 Enhancement of inductance with the increase of ferrite plate thickness $L_0 = 1.312 \mu H$

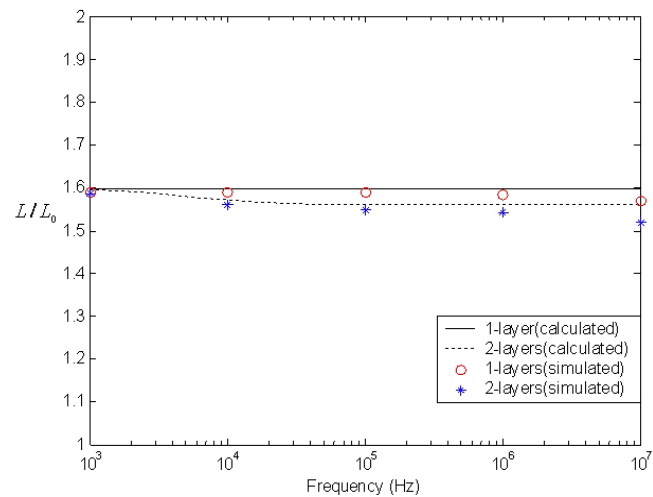


Fig. 8 (b) $t_1=0.4\text{mm}$

Fig. 8 Frequency effect of the inductance with different ferrite plate thickness

which represents this kind of loss, R_s , is calculated to be smaller than 2% of the dc resistance of the windings in the air, even when the frequency is increased to 10MHz. ($R_{s(10MHz)} = 0.0054\Omega, R_{dc} = 0.2823\Omega$). Thus, this kind of loss is not dominant compared with the ohmic loss in the windings, which is dramatically influenced by the skin effect and proximity effect at high frequency.

(iii) *comparison with the shielding effectiveness*

In order to enhance the shielding effectiveness (SE), we use the double-layered structure as the EM shield by adding a very thin copper on the bottom of ferrite [16]. This structure with 4F1 ($t_1 = 0.4mm$) and copper ($t_2 = 0.07mm$) has been proposed and the SE also has been tested for the case of single-layer and double-layer respectively. The results are shown in the Fig. 9 [19], which clearly illustrate that the EM shielding effectiveness has been enhanced by the use of the copper layer. In [19], the presence of copper layer prominently enhances the shielding effectiveness by about 20 dB to 40 dB, at the expense of only a loss of 5% of inductance value.

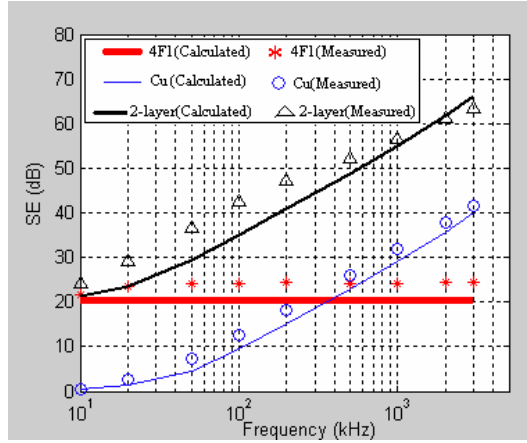


Fig. 9 Calculated and measured Shielding Effectiveness in dB [19]

In summary, when t_1 exceeds the critical value (e.g. 0.4mm for 4F1 ferrite plate), the copper sheet has little effect on the inductance of the windings (see Fig. 8(b)), even if the frequency is increased to 10MHz. But the copper sheet can improve the shielding effectiveness by more than 40dB with the same structure parameters [19]. This finding indicates a very good property of shielding effectiveness improvement without losing inductance if the thickness of the ferrite plate is beyond a critical value. This extended theory can be used to optimize the thickness of the ferrite layer in the practical work.

IV. CONCLUSION

In this paper, an extended theory on inductance calculation of planar spiral windings on a double-layered substrate is presented and verified with finite-element simulation and practical measurements. This formula is based on the physical dimensions of the spiral planar windings and the electrical and the magnetic properties of the substrate. An analysis of the variable parameters is carried out when the thickness of the ferrite plate or the frequency changes. With the help of this

extended theory, it is found that a critical value of the thickness of the ferrite layer exists for a given material of permeability. The critical thickness value decreases with increasing relative permeability of the first layer of ferrite material. This new information is important for the optimal design of the ferrite layer in the double-layered EM shield structure. The extended theory has been confirmed with simulation and measurements. It can also be reduced to the original theory if the double-layered EM shield structure is reverted to a single-layered structure.

ACKNOWLEDGEMENT

This work is supported by the Hong Kong Research Grant Council under the CERG project (CityU 114105) and the City University of Hong Kong under the Strategic Research Grant 7001761.

APPENDIX

The following procedure provides the derivation of (1)-(3) in detail, which is similar to the method described in [1]. In order to obtain the impedance formula of planar windings, the case of filamentary turns must primarily be considered as shown in Fig. 10. The filamentary turn at $z = d_1$ carries a sinusoidal current $i_\phi = I_\phi e^{j\omega t}$. The solution of Maxwell's equations must be considered in five distinct regions and [1] has presented the solution of each region about this structure.

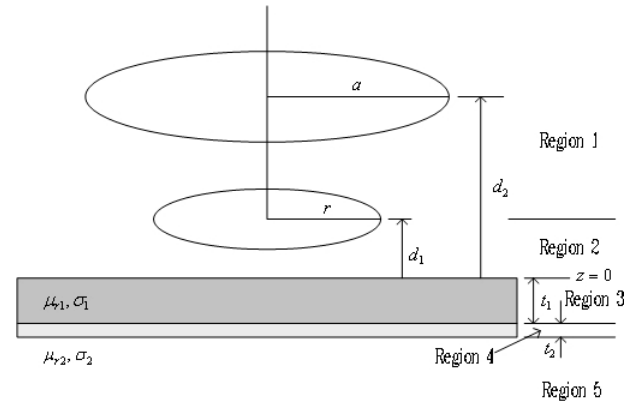


Fig. 10. Filamentary turns above a double-layer substrate

The solution of the electric field intensity E^* in each region is:

$$\text{Region 1: } z \geq d_1 \quad E^* = Ae^{-kz} \quad (A1)$$

$$\text{Region 2: } 0 \leq z < d_1 \quad E^* = Be^{kz} + Ce^{-kz} \quad (A2)$$

$$\text{Region 3: } -t_1 \leq z < 0 \quad E^* = De^{\eta z} + Fe^{-\eta z} \quad (A3)$$

$$\text{Region 4: } -(t_2 + t_1) \leq z < -t_1 \quad E^* = Ge^{\eta_2 z} + He^{-\eta_2 z} \quad (A4)$$

$$\text{Region 5: } z < -(t_2 + t_1) \quad E^* = Ie^{kz} \quad (A5)$$

There are six constants to be established on the basis of the boundary conditions. The electric field is continuous at the boundaries of $z = d_1$, $z = 0$, $z = -t_1$ and $z = -(t_1 + t_2)$:

$$Ae^{-kd_1} = Be^{kd_1} + Ce^{-kd_1} \quad (A6)$$

$$D + F = B + C \quad (A7)$$

$$De^{-\eta t_1} + Fe^{\eta t_1} = Ge^{-\eta_2 t_1} + He^{\eta_2 t_1} \quad (A8)$$

$$Ge^{-\eta_2(t_1+t_2)} + He^{\eta_2(t_1+t_2)} = Ie^{-k(t_1+t_2)} \quad (\text{A9})$$

The boundary condition on the radial component of the magnetic field intensity is given by:

$$\bar{n} \times (\bar{H}_+ - \bar{H}_-) = K_f \quad (\text{A10})$$

where \bar{n} is the unit vector normal to the plane at the boundary and K_f is the surface current density at the boundary. The radial component the magnetic field intensity is given by Maxwell's equations:

$$\frac{\partial E_\phi}{\partial z} = j\omega\mu_r\mu_0 H_r \quad (\text{A11})$$

At $z = 0$, $z = -t_1$ and $z = -(t_1 + t_2)$, there is no surface current and equating H_r at either side of the boundary gives:

$$\frac{\eta_1}{\mu_{r1}}(D - F) = k(B - C) \quad (\text{A12})$$

$$\frac{\eta_1}{\mu_{r1}}(De^{-\eta_1 t_1} - Fe^{\eta_1 t_1}) = \frac{\eta_2}{\mu_{r2}}(Ge^{-\eta_2 t_1} - He^{\eta_2 t_1}) \quad (\text{A13})$$

$$kIe^{-k(t_1+t_2)} = \frac{\eta_2}{\mu_{r2}}(Ge^{-\eta_2(t_1+t_2)} - He^{\eta_2(t_1+t_2)}) \quad (\text{A14})$$

At $z = d_1$, and in terms of $K_f^* = I_\phi a J_1(ka)$ available in [1], the final boundary condition equation could be acquired giving:

$$-Ae^{-kd_1} - Be^{kd_1} + Ce^{-kd_1} = \frac{j\omega\mu_0}{k} I_\phi a J_1(ka) \quad (\text{A15})$$

There are now eight equations in eight unknowns which can be readily solved. In terms of mutual impedance we are particularly interested in Region 1 where the electric field is

$$E^* = -j\omega\mu_0 I_\phi \frac{aJ_1(ka)}{2k} \left[e^{-k|z-d_1|} + \lambda(t_1, t_2) e^{-k(z+d_1)} \right] \quad (\text{A16})$$

$$\lambda(t_1, t_2) = \frac{\phi_1(k) + \frac{\theta(t_2) - m}{\theta(t_2) + m} e^{-2\eta_1 t_1}}{1 + \phi_1(k) \frac{\theta(t_2) - m}{\theta(t_2) + m} e^{-2\eta_1 t_1}} \quad (\text{A17})$$

Applying the inverse transform of the Fourier-Bessel integral described in [1], the mutual impedance between two filaments is obtained, in the expression of (A18), (A19) and (A20):

$$Z = j\omega M + Z_i^f \quad (\text{A18})$$

$$M = \mu_0 \pi a r \int_0^\infty J_1(kr) J_1(ka) e^{-k|d_2-d_1|} dk \quad (\text{A19})$$

$$Z_i^f = j\omega\mu_0 \pi a r \int_0^\infty J_1(kr) J_1(ka) \lambda(t_1, t_2) e^{-k(d_1+d_2)} dk \quad (\text{A20})$$

The mutual impedance between two planar windings is obtained by integrating (A20) formulas over the cross section of the conductor using the method based on the Fourier-Bessel integral transformation. The final result is shown as (1)-(12).

REFERENCE

- [1] W. G. Hurley, and M. C. Duffy, "Calculation of self and mutual impedances in planar sandwich inductors", *IEEE Transactions on Magnetics*, vol. 33, no. 3, May 1997.
- [2] W. G. Hurley, M. C. Duffy, S. O'Reilly, and S. C. O'Mathuna, "Impedance formulas for planar magnetic structures with spiral

windings", *IEEE Transactions on Industrial Electronics*, vol. 46, no. 2, April 1999.

- [3] S. Y. R. Hui, S. C. Tang, and H. S. Chung, "Coreless printed-circuit board transformer for signal and energy transfer", *Electronics Letters*, 34, (11) pp. 1052-1054, 1998
- [4] S. C. Tang, S. Y. R. Hui, and H. S. Chung, "Coreless Planar Printed-Circuit-Board (PCB) Transformers—A Fundamental Concept for Signal and Energy Transfer," *IEEE Transactions on Power Electronics*, vol. 15, no.5, pp.931-941, Sep. 2000.
- [5] T. G. Imre, W. A. Cronje, J. D. van Wyk, and J. A. Ferreira, "Loss modeling and thermal measurement in planar inductors—a case study", *IEEE Transactions on Industry Applications*, vol. 38, no. 6, pp. 1613 – 1621, Nov.-Dec. 2002.
- [6] S. Y. R. Hui, S. C. Tang, and H. S. Chung, "Optimal operation of coreless PCB transformer-isolated gate drive circuits with wide switching frequency range", *IEEE Transactions on Power Electronics*, vol. 14, no. 3, pp. 506-514, May 1999.
- [7] T. C. Neugebauer, and D. J. Perreault, "Filters with inductance cancellation using printed circuit board transformers", *IEEE Transactions on Power Electronics*, vol. 19, no. 3, pp.591-602, May 2004.
- [8] B. J. Pierquet, T. C. Neugebauer, and D. J. Perreault, "Inductance Compensation of Multiple Capacitors With Application to Common- and Differential-Mode Filters", *IEEE Transactions on Power Electronics*, vol. 21, no. 6, pp. 1815– 1824, Nov. 2006.
- [9] D. S. Lyman, T. C. Neugebauer, and D. J. Perreault, "Coupled-Magnetic Filters With Adaptive Inductance Cancellation", *IEEE Transactions on Power Electronics*, vol. 21, no. 6, pp. 1529-1540, Nov. 2006.
- [10] B. Choi, J. Nho, H. Cha, T. Ahn and S. Choi, "Design and implementation of low-profile contactless battery charger using planar printed circuit board windings as energy transfer device", *IEEE Transactions on Industrial Electronics*, vol. 51, no. 1, pp. 140-147, Feb. 2004.
- [11] J. Acero, R. Alonso, L. A. Barragan, et al., "Modeling of planar spiral inductors between two multilayer media for induction heating applications", *IEEE Transactions on Magnetics*, vol. 42, no. 11, pp. 3719-3729, Nov. 2006.
- [12] J. Acero, R. Alonso, J. M. Burdío, et al., "Analytical equivalent impedance for a planar circular induction heating system", *IEEE Transactions on Magnetics*, vol. 42, no. 1, pp. 84-86, Jan. 2006.
- [13] J. Acero, R. Alonso, J. M. Burdío, et al., "Frequency-dependent resistance in Litz-wire planar windings for domestic induction heating appliances", *IEEE Transactions on Power Electronics*, vol. 21, no. 4, pp. 856-866, Jul. 2006.
- [14] Heng-Ming Hsu, "Analytical formula for inductance of metal of various widths in spiral inductors", *IEEE Transactions on Electron Devices*, vol. 51, no. 8, pp. 1343 – 1346, Aug. 2004.
- [15] A. M. Crawford, D. Gardner, and S. X. Wang, "High-frequency microinductors with amorphous magnetic ground planes", *IEEE Transactions on Magnetics*, vol. 38, no. 5, pp. 3168-3170, Part 1, Sep. 2002.
- [16] S. Y. R. Hui, and S. C. Tang, "Planar printed-circuit-board transformers with effective electromagnetic interference (EMI) shielding", US Patent 6,501,364, 31 Dec. 2002.
- [17] S. Y. R. Hui, and W. W. C. Ho, "A new generation of universal contactless Battery Charging platform for portable Consumer Electronic equipment", *IEEE Transactions on Power Electronics*, vol. 20, no. 3, May 2005.
- [18] X. Liu, and S. Y. R. Hui, "Optimal design of a hybrid winding structure for planar contactless battery charging platform", in *Proc. IEEE IAS '06*, Oct. 2006, pp. 2568-2575.
- [19] X. Liu, and S. Y. R. Hui, "An analysis of a double-layer electromagnetic shield for a universal contactless battery charging platform", in *Proc. IEEE PESC '05*, Jun. 2005, pp. 1767-1772.